PERGAMON

www.elsevier.nl/locate/poly

Polyhedron 19 (2000) 1985–1994

POLYHEDRON

Hexanuclear manganese metallamacrocycles with tripled hydrophobic tails

Byunghoon Kwak, Hakjune Rhee, Myoung Soo Lah *

Department of Chemistry, College of Science, Hanyang University, 1271 Sa-1-dong, Ansan, Kyunggi-do 425-791, South Korea

Received 2 May 2000; accepted 4 July 2000

Abstract

A series of hexanuclear manganese(III) metallamacrocycles were synthesized using *N*-acylsalicylhydrazides (H_3xshz) (where H_3xshz = H_3ashz, *N*-acetylsalicylhydrazide; H_3pshz, *N*-propionylsalicylhydrazide; H_3hshz, *N*-hexanoylsalicylhydrazide; H_3lshz, *N*-lauroylsalicylhydrazide), where the pentadentate ligands bridged the metal ions. The triple deprotonated *N*-acylsalicylhydrazidate (xshz^{3-}) could bridge the metal ions by using a hydrazide N–N group and form the hexanuclear manganese metallamacrocycle with a hole in the center. Depending on the ligands used, the tripled hydrophobic tails of different lengths are attached at both chiral faces of the metallamacrocycles. In the complex $[Mn_6(ashz)_6(DMF)_6]$ (**2**), both sides of the hole are closed by the three methyl groups of the ligands. In the complex $[Mn_6(pshz)_6(DMF)_6]$ (**3a**), one ethyl side chain of the ligands is located inside the hole. In complexes $[Mn_6(hshz)_6(DMF)_6]$ (**4**) and $[Mn_6(lshz)_6(MeOH)_6]$ (**5**), three alternating long alkyl side chains aligned at an approximately right angle to the plane of the metallamacrocycle in one direction, while the other three alkyl side chains aligned in the opposite direction. The stability of the metallamacrocycles in the solution was addressed using ^{1}H NMR spectroscopy. Three phenyl protons of the bridging ligands in the metallamacrocycles were observed in the upfield region.

Keywords: Metallamacrocycles; Hexanuclear clusters; Manganese complexes; Pentadentate ligands; Hydrophobic aliphatic tripled tails

1. Introduction

Self-assembly is one of the most efficient methods for the synthesis of the variety of supramolecular species [1,2]. Recently, several research groups have been synthesizing and characterizing new types of inorganic cluster that can serve as inorganic counterparts of the macrocyclic organic host molecules, where the metal centers are connected by the bridging ligand. Depending on the metal ions, the bridging ligands and the additional ligands used, the self-assembled metallamacrocycles were obtained by the cyclic repeat of the metal ions and the bridging ligands. Macrocyclic squares [3], mercuracarborand cyclic species [4], metal analogue of calix[4]arene [5], and other types of metallamacrocycle [6–8] have appeared as new types of the macrocyclic inorganic host molecule, where the bidentate bridging ligands connect two metal centers.

Another type of metallamacrocycle, known as metallacrowns [9,10], has also emerged as inorganic host molecules. The tetradentate ligands, salicylhydroximate (shi^{3-}), not only serve as a bridging ligand between the metal centers, but also form the five-membered chelate ring using a hydroximate group and the six-membered chelate ring using a iminophenolate group. The chelation gave the metallamacrocycles additional stabilization. Depending on the chelation mode of the ligands around the metal center, the metal centers of the metallamacrocycle could have two different configurations,

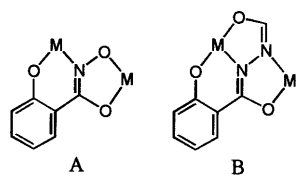

Fig. 1. (A) Binding site of shi^{3-}: 6-, 5-membered chelating rings. (B) Binding sites of fshz^{3-}: 6-, 5-, 5-membered chelating rings.

* Corresponding author. Tel.: +82-31-400-5496; fax: +82-31-400-3863.

E-mail address: mslah@email.hanyang.ac.kr (M.S. Lah).

0277-5387/00/$ - see front matter
PII: S0277-5387(00)00499-X

the planar configuration and the propeller configuration [9a,c].

We have recently synthesized a new type of metallamacrocycle [11], where the pentadentate ligand, *N*-formylsalicylhydrazide (H_3fshz), bridged the metal ions using a hydrazide N–N group (instead of a hydroximate N–O group of the salicylhydroximate) and formed three chelate rings in each metal center (Fig. 1). In addition, the chelation mode of the ligands enforced the metal centers only into the propeller configuration. The metallamacrocycle $[Mn(III)_6(fshz)_6(MeOH)_6]$ (**1**) [11], prepared by using a trianionic pentadentate ligand $fshz^{3-}$, has a large, vacant and hydrophobic hole in the center of the metallamacrocycle. The chiralities of the metal center in metallamacrocycle **1** alternate between Λ and Δ forms. As a result of the alternation, two faces of the donut-shaped hexanuclear manganese metallamacrocycle have opposite chiralities to each other.

In this study, we synthesized a series of pentadentate ligands with various lengths of hydrophobic alkyl chains and their corresponding hexanuclear manganese metallamacrocycles. We report here the general method of synthesizing the series of pentadentate ligands and the features of the corresponding hexanuclear manganese metallamacrocycles with tripled hydrophobic tails. These metallamacrocycles have been characterized using X-ray crystallography and spectroscopic methods.

2. Experimental

2.1. Materials

The following were used as received with no further purification: Salicylhydrazide, dimethylsulfoxide-d_6 (DMSO) and acetone-d_6, acetic anhydride, propionic anhydride, hexanoyl chloride, lauroyl chloride and triethylamine from Aldrich, Inc.; manganese acetate tetrahydrate from Yakuri; acetone, diethylether, chloroform, hexane, methanol (MeOH), ethanol (EtOH), dimethylformamide (DMF) and tetrahydrofuran (THF) from Carlo Erba.

2.2. Instrumentation

The Elemental Analysis Laboratory of the Korean Institute of Basic Science performed C, H, N and Mn determinations. Infrared spectra were recorded as KBr pellets in the range 4000–600 cm^{-1} on a Bio-Rad FTIR spectrometer. Absorption spectra were obtained using a Perkin Elmer Lambda spectrometer. NMR spectra were obtained using a Varian-300 spectrometer. Positive-ion FAB mass spectra were obtained using a JEOL HX110A/HX110A tandem mass spectrometer in a 3-nitrobenzyl alcohol matrix. Room temperature (r.t.) magnetic susceptibilities of well-ground solid samples were measured by using an Evans balance. The measurements were calibrated against a $Hg[Co(SCN)_4]$ standard.

2.3. Synthesis

2.3.1. Ligand synthesis

2.3.1.1. N-Acetylsalicylhydrazide (H_3ashz). Salicylhydrazide (2.017 g, 13.3 mmol) was added to acetic anhydride (8.00 ml) at an ambient temperature. A white suspension was immediately obtained. The suspension was diluted with diethylether, filtered, and rinsed with diethylether (2.453 g, 95% yield). M.p. = 174–176°C. IR (KBr pellet): 3187, 1605, 1573, 1487, 1235, 753 cm^{-1}. ^{1}H NMR (300 MHz, DMSO-d_6): δ 11.90, 10.54, 10.18 (br s, br s, s, 3H, Hs at amides and phenolic OH), 7.90 (dd, 1H, $J = 7.9$, 1.5 Hz, H at phenyl), 7.44 (td, 1H, $J = 7.8$, 1.6 Hz, H at phenyl), 7.03–6.91 (m, 2H, Hs at phenyl), 1.96 (s, 3H, H at methyl). ^{13}C NMR (75.5 MHz, DMSO-d_6): δ 168.29, 167.06, 159.21, 134.36, 128.78, 119.39, 117.65, 115.02, 20.81. *Anal.* Calc. for $C_9H_{10}N_2O_3$: C, 55.67; H, 5.19; N, 14.43. Found: C, 55.74; H, 5.22; N, 14.69%.

2.3.1.2. N-Propionylsalicylhydrazide (H_3pshz). The ligand, *N*-propionylsalicylhydrazide was prepared in an analogous manner to that used for *N*-acetylsalicylhydrazide. Propionic anhydride (8.00 ml) was used. 91% yield. M.p. = 148–151°C. IR (KBr pellet): 3333, 3302, 3201, 2976, 1675, 1640, 1607, 1485, 1236, 752 cm^{-1}. ^{1}H NMR (300 MHz, DMSO-d_6): δ 11.93, 10.54, 10.12 (s, s, s, 3H, Hs at amides and phenolic OH), 7.91 (dd, 1H, $J = 7.9$, 1.5 Hz, H at phenyl), 7.44 (td, 1H, $J = 7.7$, 1.5 Hz, H at phenyl), 6.99–6.91 (m, 2H, Hs at phenyl), 2.25 (q, 2H, $J = 7.6$ Hz, H at –CH_2–), 1.09 (t, 3H, $J = 7.6$ Hz, H at –CH_3). ^{13}C NMR (75.5 MHz, DMSO-d_6): δ 172.14, 167.19, 159.27, 134.35, 128.71, 119.36, 117.66, 114.98, 26.81, 9.96. *Anal.* Calc. for $C_{10}H_{12}N_2O_3$: C, 57.69; H, 5.81; N, 13.45. Found: C, 57.48; H, 5.68; N, 12.75%.

2.3.1.3. N-Hexanoylsalicylhydrazide (H_3hshz). Hexanoyl chloride (2.76 ml, 19.7 mmol) was added to a solution of chloroform (100 ml) containing water (0.36 ml, 19.7 mmol) and triethylamine (5.5 ml, 39.4 mmol) at 0°C. The reaction mixture was slowly warmed to ambient temperature. Another hexanoyl chloride (2.76 ml, 19.7 mmol) was added to the mixture. Then, salicylhydrazide (2.500 g, 16.4 mmol) was added to the reaction mixture. The resulting reaction mixture was stirred at ambient temperature for 1 day. The white suspension was diluted with hexane (200 ml), filtered, and rinsed with water (50 ml × 3) and hexane (50 ml × 5). 3.450 g of the product was obtained (84% yield). M.p. = 163–

165°C. IR (KBr pellet): 3323, 3195, 2963, 2935, 1610, 1576, 1490, 1235, 756 cm^{-1}. ^1H NMR (300 MHz, DMSO-d_6): δ 11.89, 10.48, 10.07 (s, s, s, 3H, Hs at amides and phenolic OH), 7.83 (dd, 1H, $J = 7.9$, 1.3 Hz, H at phenyl), 7.36 (td, 1H, $J = 7.7$, 1.4 Hz, H at phenyl), 6.95–6.83 (m, 2H, Hs at phenyl), 2.14 (t, 2H, $J = 7.4$ Hz, H at $-CH_2-$), 1.49 (m, 2H, H at $-CH_2-$), 1.22 (m, 4H, H at $-CH_2-CH_2-$), 0.80 (t, 3H, $J = 6.8$ Hz, H at $-CH_3$). ^{13}C NMR (75.5 MHz, DMSO-d_6): δ 172.57, 168.41, 160.69, 135.57, 129.90, 120.55, 118.87, 116.10, 34.70, 32.46, 26.29, 23.43, 15.40. *Anal.* Calc. for $C_{13}H_{18}N_2O_3$: C, 62.38; H, 7.25; N, 11.90. Found: C, 62.17; H, 7.18; N, 11.73%.

2.3.1.4. N-Lauroylsalicylhydrazide (H_3lshz). The ligand *N*-lauroylsalicylhydrazide was prepared in an analogous manner to that used for *N*-hexanoylsalicylhydrazide. Lauroyl chloride (2.76 ml, 19.7 mmol) was used. 93% yield. M.p. = 145–147°C. IR (KBr pellet): 3328, 3195, 2919, 2850, 1604, 1576, 1490, 1234, 751 cm^{-1}. ^1H NMR (300 MHz, DMSO-d_6): δ 11.97, 10.56, 10.15 (br s, br s, s, 3H, Hs at amides and phenolic OH), 7.91 (dd, 1H, $J = 7.9$, 1.5 Hz, H at phenyl), 7.44 (td, 1H, $J = 7.8$, 1.5 Hz, H at phenyl), 7.00–6.90 (m, 2H, Hs at phenyl), 2.22 (t, 2H, $J = 7.3$ Hz, H at $-CH_2-$), 1.54 (m, 2H, H at $-CH_2-$), 1.26 (m, 16H, H at $-(CH_2)_8-$), 0.86 (t, 3H, $J = 6.6$ Hz, H at $-CH_3$). ^{13}C NMR (75.5 MHz, DMSO-d_6): δ 171.28, 167.12, 159.48, 134.32, 128.69, 119.30, 117.64, 114.89, 33.53, 31.70, 29.42, 29.35, 29.18, 29.13, 28.96, 25.43, 22.49.14.28. *Anal.* Calc. for $C_{19}H_{30}N_2O_3$: C, 68.23; H, 9.04; N, 8.38. Found: C, 67.97; H, 9.02; N, 8.39%.

2.3.2. Synthesis of metallamacrocycles

*2.3.2.1. [Mn(fshz)(MeOH)]$_6$ (**1**).* The metallamacrocycle, [Mn(fshz)(MeOH)]$_6$, was synthesized as previously described [11]. ^1H NMR (acetone-d_6): δ −10.14, −21.64, −34.94 (Hs at phenyl); 3.03 (Hs for H_2O).

*2.3.2.2. [Mn(ashz)(DMF)]$_6$ (**2**).* A 0.588 g (3.0 mmol) sample of *N*-acetylsalicylhydrazide was dissolved in 30 ml of DMF and 0.735 g (3.0 mmol) of manganese(II) acetate tetrahydrate was dissolved in 30 ml of DMF in another flask. The two solutions were mixed and the combined solution was allowed to stand for 4 days, whereupon dark brown rectangular crystals were obtained (0.935 g, 90.7% yield). *Anal.* Calc. for [Mn(ashz)(DMF)]$_6$·2DMF ($C_{78}H_{98}Mn_6N_{20}O_{26}$) (fw = 2061.38): C, 45.45; H, 4.79; Mn, 15.99; N, 13.59. Found: C, 45.32; H, 5.20; Mn, 16.55; N, 14.25%. ^1H NMR (acetone-d_6): δ −10.03, −20.40, −33.12 (Hs at phenyl); 37.94 (H at C9); 8.01, 2.95, 2.79 (Hs for DMF); 2.99 (Hs for H_2O). FABMS, m/z: $[Mn_6(ashz)_6 + H]^+$, 1477.6. UV–Vis ($CHCl_3$) $\lambda_{max}(\varepsilon)$: 249 nm (36 500 M^{-1} cm^{-1}); 298 nm (20 100 M^{-1} cm^{-1}); 364 nm (10 600 M^{-1} cm^{-1}). μ_{eff}: 11.84 μ_B (4.83 μ_B/metal).

*2.3.2.3. [Mn(pshz)(DMF)]$_6$ (**3a**).* A 0.365 g (2.0 mmol) sample of *N*-propionylsalicylhydrazide was dissolved in 15 ml of DMF and 0.49 g (2.0 mmol) of manganese(II) acetate tetrahydrate was dissolved in 15 ml of DMF in another flask. The two solutions were mixed and the combined solution was allowed to stand for 4 days, whereupon dark brown rectangular crystals were obtained (0.58 g, 87.0% yield). *Anal.* Calc. for [Mn(pshz)(DMF)]$_6$ ($C_{78}H_{96}Mn_6N_{18}O_{24}$) ($F_w = 1999.35$): C, 46.86; H, 4.84; Mn, 16.49; N, 12.61. Found: C, 46.56; H, 5.58; Mn, 16.18; N, 13.23%. ^1H NMR (acetone-d_6): δ −2.76(br); −10.10, −20.26, −32.90 (Hs at phenyl); 49.90 (H at C9); 8.10, 2.99, 2.82 (Hs for DMF); 3.11 (Hs for H_2O). UV–Vis (acetone) $\lambda_{max}(\varepsilon)$: 328 nm (27400 M^{-1} cm^{-1}); 372 nm (17 500 M^{-1} cm^{-1}); 467 nm (2460 M^{-1} cm^{-1}). μ_{eff}: 11.13 μ_B (4.55 μ_B/metal).

*2.3.2.4. [Mn(pshz)(EtOH)]$_6$ (**3b**).* A 0.10 g (0.5 mmol) sample of *N*-propionylsalicylhydrazide was dissolved in 5 ml of DMF and 0.123 g (0.5 mmol) of manganese(II) acetate tetrahydrate was dissolved in 5 ml of DMF in another flask. The two solutions were mixed and the combined solution was allowed to stand for 4 days, whereupon dark brown rectangular crystals were obtained (0.10 g, 67% yield). *Anal.* Calc. for [Mn_6(pshz)$_6$(EtOH)$_5$] ($C_{70}H_{84}Mn_6N_{12}O_{23}$) ($F_w = 1791.13$): C, 46.94; H, 4.73; Mn, 18.40; N, 9.38. Found: C, 46.25; H, 4.51; Mn, 18.46; N, 9.36%. UV–Vis (THF) $\lambda_{max}(\varepsilon)$: 239 nm (233 000 M^{-1} cm^{-1}); 278 nm (193 000 M^{-1} cm^{-1}); 327 nm (45 600 M^{-1} cm^{-1}); 369 nm (26 700 M^{-1} cm^{-1}); 439 nm (3850 M^{-1} cm^{-1}); 739 nm (2640 M^{-1} cm^{-1}).

*2.3.2.5. [Mn(hshz)(DMF)]$_6$ (**4**).* A 0.250 g (1.0 mmol) sample of *N*-hexanoylsalicylhydrazide was dissolved in 15 ml of DMF and 0.245 g (1.0 mmol) of manganese (II) acetate tetrahydrate was dissolved in 15 ml of DMF in another flask. The two solutions were mixed and the combined solution was allowed to stand for 5 days, whereupon dark brown rectangular crystals were obtained (0.352 g, 93.8% yield). *Anal.* Calc. for [Mn(hshz)(DMF)]$_6$ ($Mn_6C_{96}H_{132}N_{18}O_{24}$) ($F_w$ = 2251.84): C, 51.21; H, 5.91; Mn, 14.64; N, 11.20. Found: C, 51.04; H, 5.88; Mn, 14.00; N, 11.25. ^1H NMR (acetone-d_6): δ -12.0(shoulder); −10.63, −20.61, −32.56 (Hs at phenyl); 54.73 (H at C9); 8.43, 3.102, 2.926 (Hs for DMF); 3.351 (Hs for H_2O); 1.30, 0.51 (Hs for alkyl chains). UV–Vis (THF) $\lambda_{max}(\varepsilon)$: 239 nm (247 000 M^{-1} cm^{-1}); 278 nm (208 000 M^{-1} cm^{-1}); 369 nm (24 000 M^{-1} cm^{-1}); 456 nm (4060 M^{-1} cm^{-1}). UV − Vis (acetone) $\lambda_{max}(\varepsilon)$: 326 nm (31 000 M^{-1} cm^{-1}); 374 nm (19 200 M^{-1} cm^{-1}); 458 nm (2200 M^{-1} cm^{-1}). μ_{eff}: 11.59 μ_B (4.73 μ_B/metal).

*2.3.2.6. [Mn(lshz)(MeOH)]$_6$ (**5**).* A 0.668 g (2.0 mmol) sample of *N*-lauroylsalicylhydrazide was dissolved in 80 ml of MeOH and 0.490 g (2.0 mmol) of manganese(II) acetate tetrahydrate was dissolved in 20 ml of MeOH in another flask. When the two solutions were mixed precipitate formed immediately. After a day of stirring, the solution was filtered to obtain 0.56 g of undissolved powder. The filtrate was allowed to stand for 3 days, whereupon dark brown rectangular crystals were obtained (0.10 g, 11.9% yield). The undissolved powder obtained from the early stage of the reaction was added to 200 ml of MeOH. After a week of the stirring, most of powders were dissolved. Slow evaporation of the solution yielded the same dark rectangular crystals (0.34 g, 40.6% yield). *Anal.* Calc. for [Mn(lshz)(MeOH)]$_6$ ($Mn_6C_{120}H_{186}N_{12}O_{24}$) ($F_w$ = 2510.49): C, 57.41; H, 7.47; Mn, 13.13; N, 6.70. Found: C, 57.06; H, 8.07; Mn, 13.77; N, 7.03%. ^{1}H NMR (acetone-d_6): δ −10.44, −20.35, −31.18 (Hs at phenyl); 52.95 (H at C9); 3.837(Hs for H_2O); 5.792, 1.296, 0.915 (Hs for alkyl chains). UV–Vis (THF) $\lambda_{max}(\varepsilon)$: 239 nm (249 000 M^{-1} cm^{-1}); 278 nm (214 000 M^{-1} cm^{-1}); 368 nm (24 000 M^{-1} cm^{-1}); 466 nm (4020 M^{-1} cm^{-1}); 742 nm (360 M^{-1} cm^{-1}). UV–Vis (acetone) $\lambda_{max}(\varepsilon)$: 328 nm (34 200 M^{-1} cm^{-1}); 375 nm (21 900 M^{-1} cm^{-1}); 465 nm (3500 M^{-1} cm^{-1}). μ_{eff}: 11.63 μ_B (4.75 μ_B/metal).

2.4. Crystallographic data collection and refinement of structures

Because crystals of **2**–**5** lose their structural solvents of crystallization within 1 min, they were mounted in a glass capillary with the mother liquor to prevent the loss of the structural solvents during data collection. Preliminary examination and data collection for crystals of **2**–**4** were performed with Mo Kα radiation (λ = 0.71069 Å) on an Enraf–Nonius CAD4 computer-controlled κ-axis diffractometer equipped with a graphite crystal, incident-beam monochromator. Cell constants and orientation matrices for data collection were obtained from least-squares refinement, using the setting angles of 25 reflections. Data were collected at r.t. using the ω scan technique. Three standard reflections were monitored every hour, but no intensity variations were monitored. Lorentz and polarization corrections were applied to the data; however, no corrections were made for absorption. Preliminary examination and data collection for the crystal of **5** were performed with Mo Kα radiation (λ = 0.71069 Å) on a Siemens SMART CCD equipped with a graphite crystal, incident-beam monochromator. Data were collected at r.t. Lp correction and absorption correction were applied to the data. All structures were solved by direct methods using SHELXS-86 [12] and refined by full-matrix least-squares calculations with SHELX-97 [13].

*2.4.1. Complex [Mn(ashz)(DMF)]$_6$ (**2**).*

All non-hydrogen atoms except one solvent molecule were refined anisotropically; hydrogen atoms were allowed to ride on geometrically ideal positions with isotropic temperature factors 1.2 times those of the attached non-hydrogen atoms. One DMF molecule coordinated to the ring metal ion is statically disordered. This disordered site was refined with two partially occupied DMF molecules (0.47 occupancy site: O4C, C101, N3C, C111, C121; 0.53 occupancy site: O4C, C102, N3C, C112, C122). Two solvent sites were identified; one of them performed very poorly. Refinement without any geometrical restraint or with disordered modelling produced bad geometry. So the geometry of this solvent molecule was restrained the same as the geometry of the other solvent molecule.

*2.4.2. Complex [Mn(pshz)(DMF)]$_6$ (**3a**).*

All non-hydrogen atoms (except disordered sites) were refined anisotropically; hydrogen atoms were allowed to ride on geometrically ideal positions with isotropic temperature factors 1.2 times those of the attached non-hydrogen atoms. All ethyl side chains of the ligands were disordered. These disordered sites were refined with partial occupancy. One disordered ethyl side chain showed abnormal bond distances (C9A–C10A 1.73; C9A–C11A 1.86 Å). The restrained refinement with an ideal geometry gave similar result. Two solvent sites were identified, one of them performed very badly. Refinement without any geometrical restraint or with disordered modelling produced bad geometry. So the geometry of this solvent molecule was restrained the same as the geometry of the other solvent molecule.

*2.4.3. Complex [Mn(hshz)(DMF)]$_6$ (**4**).*

All non-hydrogen atoms were refined anisotropically; hydrogen atoms were allowed to ride on geometrically ideal positions with isotropic temperature factors 1.2 times those of the attached non-hydrogen atoms. Two solvent sites were identified; one of which yield an abnormal bond distance (1.78 Å) between O1DE–C1DE. So the geometry of this solvent molecule was restrained the same as the geometry of the other solvent molecule.

*2.4.4. Complex [Mn(lshz)(MeOH)]$_6$ (**5**).*

All non-hydrogen atoms were refined anisotropically; hydrogen atoms were allowed to ride on geometrically ideal positions with isotropic temperature factors 1.2 times those of the attached non-hydrogen atoms. In the crystal structures, only portions of the long alkyl side chains could be identified in the difference Fourier map. The remaining terminal carbon atoms were disordered. During the least-squares refinement of the crystal **5**, the alkyl side chains of the ligands were restrained as an

Table 1
Crystallographic data for $[Mn(III)(ashz)(DMF)]_6 \cdot 4DMF$ (**2**), $[Mn(III)(pshz)(DMF)]_6 \cdot 4DMF$ (**3a**), $[Mn(III)(hshz)(DMF)]_6 \cdot 4DMF$ (**4**), $[Mn(III)(lshz)(MeOH)]_6 \cdot 4.67MeOH$ (**5**)

	Complex **2**	Complex **3a**	Complex **4**	Complex **5**
Formula	$C_{42}H_{56}Mn_3N_{11}O_{14}$	$C_{45}H_{62}Mn_3N_{11}O_{14}$	$C_{54}H_{80}Mn_3N_{11}O_{14}$	$C_{187}H_{307}Mn_9N_{18}O_{43}$
Formula weight	1103.80	1145.88	1272.11	3989.97
Space group	$P\bar{1}$	$P\bar{1}$	$P\bar{1}$	$P\bar{1}$
Z	2	2	2	6
a (Å)	12.866(2)	13.039(2)	14.685(2)	16.4398(3)
b (Å)	14.608(2)	14.691(3)	15.737(2)	28.0779(5)
c (Å)	15.957(2)	16.238(4)	16.178(2)	28.6136(5)
α (°)	63.94(1)	110.64(2)	61.708(6)	118.772(1)
β (°)	73.82(2)	94.85(2)	81.529(8)	93.650(1)
γ (°)	76.46(2)	109.43(2)	75.808(8)	100.871(1)
V (Å^3)	2565.7(6)	2672.3(9)	3189.5(6)	11185.0(3)
Max θ value (°)	20	20	20	20
Crystal size (mm)	$0.54 \times 0.40 \times 0.30$	$0.70 \times 0.32 \times 0.28$	$0.50 \times 0.40 \times 0.10$	$0.60 \times 0.25 \times 0.20$
Number reflections collected	4790	4986	5933	34 154
Number independent reflections	4790[$R_{int} = 0.00$]	4986[$R_{int} = 0.00$]	5930[$R_{int} = 0.008$]	20 479[$R_{int} = 0.072$]
Goodness-of-fit on F^2	1.121	1.086	1.081	1.011
Final R [$I > 2\sigma(I)$]	$R_1 = 0.0697$ [a]	$R_1 = 0.0727$	$R_1 = 0.0535$	$R_1 = 0.0914$
	$wR_2 = 0.1727$ [b]	$WR_2 = 0.1784$	$wR_2 = 0.1283$	$wR_2 = 0.2607$
R (all data)	$R_1 = 0.0932$	$R_1 = 0.1293$	$R_1 = 0.0924$	$R_1 = 0.1512$
	$wR_2 = 0.1866$	$WR_2 = 0.2198$	$wR_2 = 0.1541$	$wR_2 = 0.3107$

[a] $R_1 = \Sigma(|F_o| - |F_c|)/\Sigma|F_o|$.
[b] $wR_2 = [\Sigma w(F_o^2 - F_c^2)^2/\Sigma wF_o^4]^{1/2}$.

ideal geometry. Seven solvent sites were identified and refined as methanol molecules but some of them might be part of the unconnected long alkyl side chains.

Crystal and intensity data are given in Table 1.

3. Results and discussion

In this study, a series of potential pentadentate ligands, *N*-acylsalicylhydrazides (H_3xshz) (–$COCH_3$, *N*-acetylsalicylhydrazide; –$COCH_2CH_3$, *N*-propionylsalicylhydrazide; –$CO(CH_2)_2CH_3$, *N*-hexanoylsalicylhydrazide; and, –$CO(CH_2)_{10}CH_3$, *N*-lauroylsalicylhydrazide) were synthesized by the coupling of the salicylhydrazide and the corresponding acyl chloride or acyl anhydrides. The triple deprotonated *N*-acylsalicylhydrazidate (xshz^{3-}) with a linear aliphatic chain were able to bridge the metal ions using a hydrazide N–N group and form the isostructural hexanuclear manganese metallamacrocycle. Depending on the ligands used, the tripled hydrophobic aliphatic tails of different lengths are attached at both chiral faces of the hexanuclear manganese metallamacrocycle (Fig. 2).

3.1. Crystal structure of $[Mn(ashz)(DMF)]_6$ (2)

Hexanuclear manganese metallamacrocycle $[Mn(ashz)(DMF)]_6$, **2** were able to be synthesized using manganese(II) acetate tetrahydrate as a metal source and ashz^{3-} as a trianionic pentadentate ligand. An ORTEP diagram of complex **2** is shown in Fig. 3. This neutral hexanuclear manganese metallamacrocycle is similar to the previously reported hexanuclear manganese metallamacrocycle $[Mn(fshz)(DMF)]_6$ (**1**) (Tables 2 and 3) [11]. Complex **2** with noncrystallographic local pseudo-C_{3i} symmetry is in the crystallographic inversion center. As in complex **1**, the pentadentate ligand *N*-acetylsalicylhydrazidate also bridges the ring metal ions using a hydrazide N–N group. An iminophenolate group (O1 and N1 atoms) and an iminoacetyl group (N1 and O3 atoms) of the ligand are coordinated to the metal ion in the meridional mode to form the six-membered and five-membered chelating rings. A hydrazidate group (O2 and N2 atoms) occupies two of the three remaining coordination sites of the octahedral

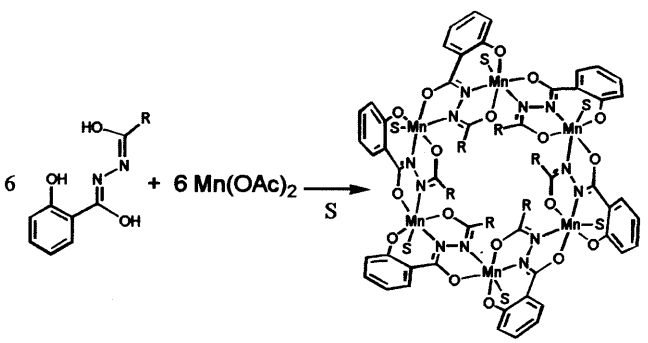

Fig. 2. Synthesis of metallamacrocycles.

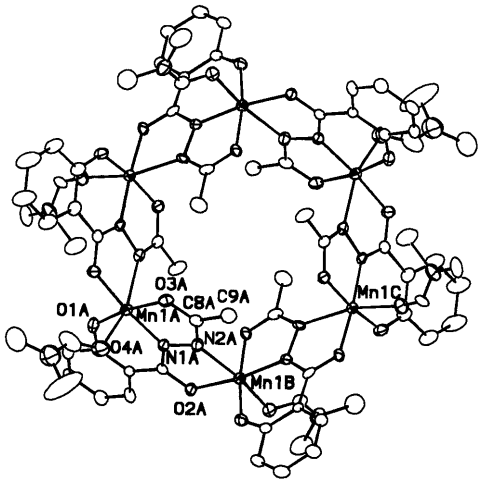

Fig. 3. An ORTEP drawing of complex **2**, $[Mn(ashz)(DMF)]_6$. The complex is in the crystallographic inversion center. A, B, and C in manganese ions could be related to each other by using a noncrystallographic S_6 symmetry operation. Hydrogen atoms have been omitted for clarity.

Table 2
Selected bond lengths (Å) [a] and angles (°) [a] for **1**, **2**, **3a**, **4** and **5**

	1 [b]	**2**	**3a**	**4**	**5**
Mn1–O1	1.852	1.851	1.859	1.852	1.858
Mn1–O2 [c]	1.967	1.967	1.971	1.973	1.967
Mn1–O3	1.945	1.929	1.925	1.915	1.923
Mn1–N1	1.929	1.942	1.93	1.935	1.932
Mn1–O4	2.233	2.248	2.260	2.239	2.268
Mn1–N2 [c]	2.246	2.251	2.27	2.265	2.251
O1A–Mn1A–O2C [c]	94.6	96.5	96.2	95.7	96.5
O1A–Mn1A–O3A	169.9	170.7	170.3	170.0	170.5
O1A–Mn1A–O4A	92.1	91.6	91.3	91.4	89.7
O1A–Mn1A–N1A	90.5	90.8	90.6	90.5	91.0
O1A–Mn1A–N2C [c]	96.7	93.9	93.1	95.7	94.4
O2C [b]–Mn1A–O3A	95.0	92.7	93.4	93.9	92.5
O2C [b]–Mn1A–O4A	83.6	86.8	86.0	85.8	86.7
O2C [b]–Mn1A–N1A	172.7	172.5	173.0	173.4	172.3
O2C [b]–Mn1A–N2C [c]	74.7	75.1	74.3	74.3	74.8
O3A–Mn1A–O4A	86.0	88.5	88.3	86.5	88.5
O3A–Mn1A–N1A	80.2	80.1	79.7	80.1	80.0
O3A–Mn1A–N2C[c]	88.7	88.9	89.7	89.5	90.2
O4A–Mn1A–N1A	101.5	94.6	95.0	95.9	94.0
O4A–Mn1A–N2C[c]	157.0	161.3	159.3	159.2	161.0
N1A–Mn1A–N2C[c]	99.6	102.9	104.3	103.4	104.1

[a] The geometry data are the average values of the bond distances and angles related by the noncrystallographic S_6 symmetry operation.
[b] Ref. [11].
[c] Symmetry transformation used to generate equivalent atoms: $1-x, -y+2, -z$

manganese ions to form the five-membered chelating ring. A solvent molecule DMF (O4 atom), coordinated at the Jahn–Teller elongation axis, finishes the octahedral geometry of the manganese ion (Table 2). The binding mode of the ligand enforces the stereochemistry of the metal ions only into a propeller configuration in the complex **2**. The resulting chiralities of the metal centers in complex **2** alternate between Λ and Δ forms. The alternation of the chiralities of the metal centers generates two chiral faces with opposite chiralities in the hexanuclear manganese metallamacrocycle. Complex **2** also has a vacant, hydrophobic hole in the center of the metallamacrocycle. The approximate dimensions of the hydrophobic hole are similar to those in the previously reported complex **1**, $[Mn(fshz)(DMF)]_6$ (Table 3). However, in complex **2** the entrance of the hole at each face is closed by three methyl groups of the *N*-acetyl side chains of the ligands. The diameter of the entrance of the hole, formed by the pseudo-C_3 symmetry-related three methyl carbon atoms (C9), is about 1.3 Å smaller than that of the entrance of the hole formed by the pseudo-C_3 symmetry-related three C8 carbon atoms (Table 3).

3.2. Crystal structure of $[Mn(pshz)(DMF)]_6$ (3a)

Hexanuclear manganese metallamacrocycle $[Mn(pshz)(DMF)]_6$ (**3a**) could be synthesized using manganese(II) acetate tetrahydrate as a metal source and $pshz^{3-}$ as a trianionic pentadentate ligand. An ORTEP diagram of complex **3a** is shown in Fig. 4. This neutral hexanuclear manganese metallamacrocycle is also similar to the previously reported hexanuclear manganese metallamacrocycle $[Mn(fshz)(DMF)]_6$ (**1**) and $[Mn(ashz)(DMF)]_6$ (**2**). Complex **3a** with noncrystallographic local pseudo-C_{3i} symmetry is also in the crystallographic inversion center. In the crystal structure, ethyl side chains of the ligands (three ethyl side chains in the asymmetric unit) are disordered. In the complex **3a**, only one entrance of the hole is blocked by three ethyl groups of the *N*-propionyl side chains of the ligands. At the other entrance of the hole, one ethyl group is located on the inside of the hole and the remaining two ethyl groups are at the face of the hole. When the ethyl group located in the inside of the hole was omitted during crystallographic refinement, the difference Fourier map showed about 1.5 residual electron density per $Å^2$. In addition, the hole of the metallamacrocycle

Table 3
Selected lengths (Å) and hole sizes (Å) for **1**, **2**, **3a**, **4** and **5**

	1 [a]	**2**	**3**	**4**	**5**
Mn1A···Mn1B	4.805	4.819	4.891	4.880	4.877
Mn1A···Mn1C	8.031	8.208	8.256	8.183	8.268
Hole size [b]	6.89	7.10	7.15	7.07	7.17
C8A···C8C	5.026	5.226	5.405	5.235	5.355
Hole size	2.70	2.93	3.14	2.94	3.08

[a] Ref. [11].
[b] The hole was formed by the three pseudo-C_3 symmetry-related atoms and the size of the hole was calculated by the subtraction of the Van der Waals radii of the constituting atoms.

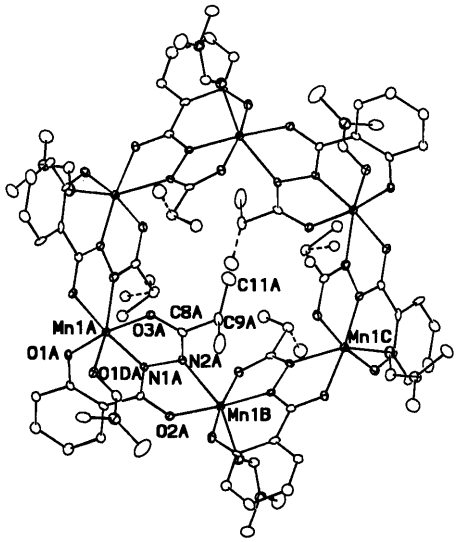

Fig. 4. An ORTEP drawing of complex **3a**, $[Mn(pshz)(DMF)]_6$. The complex is in the crystallographic inversion center. A, B, and C in manganese ions could be related to each other by using a noncrystallographic S_6 symmetry operation. The dotted lines are for the disordered ethyl groups. Hydrogen atoms have been omitted for clarity.

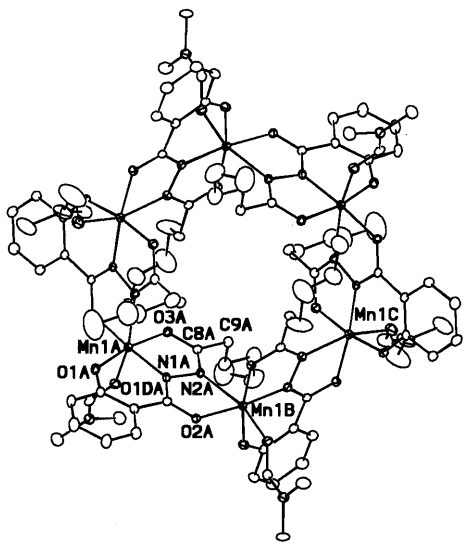

Fig. 5. An ORTEP drawing of complex **4**, $[Mn(hshz)(DMF)]_6$. The complex is in the crystallographic inversion center. A, B, and C in manganese ions could be related to each other by using a noncrystallographic S_6 symmetry operation. Hydrogen atoms have been omitted for clarity.

expanded slightly. The diameter of the entrance formed by the pseudo C_3 symmetry related three C8 atoms in the complex **3a** increased approximately 0.4 Å compared to the corresponding diameter in the complex **1** (Table 3). The incorporation of the ethyl group resulted in the expansion of the hole. This shows that the hexanuclear manganese metallamacrocycle has some degree of flexibility.

3.3. Crystal structure of $[Mn(hshz)(DMF)]_6$ (4)

Hexanuclear manganese metallamacrocycle $[Mn(hshz)(DMF)]_6$ (**4**) could be synthesized using manganese(II) acetate tetrahydrate as a metal source and $hshz^{3-}$ as a trianionic pentadentate ligand. An ORTEP diagram of complex **4** is shown in Fig. 5. The complex has two sets of tripled hydrophobic tails at each face of the donut shaped metallamacrocycles. In the crystal structure, three alternating pentyl side chains aligned at an approximately right angle to the plane of the metallamacrocycle in one direction, while the other three alternating pentyl side chains aligned in the opposite direction (Fig. 6).

3.4. Crystal structure of $[Mn(lshz)(MeOH)]_6$ (5)

Hexanuclear manganese metallamacrocycle $[Mn(lshz)(MeOH)]_6$ (**5**) could be synthesized using manganese(II) acetate tetrahydrate as a metal source and $lshz^{3-}$ as a trianionic pentadentate ligand. The crystal structure showed three crystallographically independent, but chemically identical, molecules. In the crystal structure, only a portion of the long alkyl side chains could be identified. Depending on the alkyl side chains in the three crystallographically independent molecules, three to seven carbon atoms among eleven could be found in the difference Fourier map. The remaining terminal carbon atoms were disordered. An ORTEP drawing of one of these molecules (complex **5**) is shown in Fig. 7. The three alternating hydrophobic alkyl chains aligned at an approximately right angle to the plane of the metallamacrocycle, and the other three alkyl chains aligned in the opposite direction as in

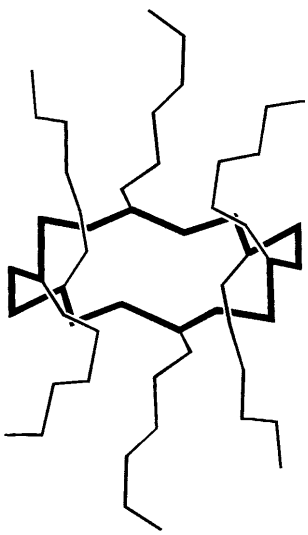

Fig. 6. Side view of complex **4**, $[Mn(hshz)(DMF)]_6$. Cyclic $(Mn–N–N–)_6$ linkage is drawn in bold. The alternating side chains aligned at an approximately right angle to the plane of the metallamacrocycle.

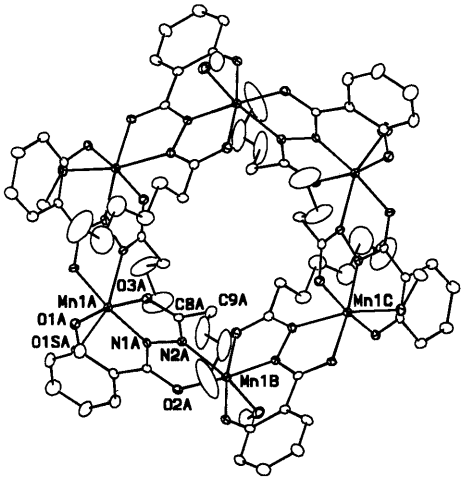

Fig. 7. An ORTEP drawing of complex **5**, $[Mn(lshz)(MeOH)]_6$. Only parts of the alkyl chains could be identified in the difference Fourier map. A, B and C in manganese ions could be related to each other by using a noncrystallographic S_6 symmetry operation. Hydrogen atoms have been omitted for clarity.

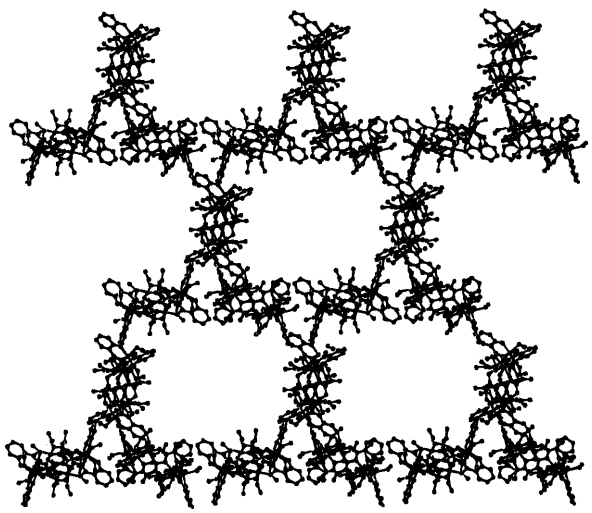

Fig. 8. Packing diagram of complex **5**, $[Mn(lshz)(MeOH)]_6$. Complex **5** serves as unit for the gigantic hexagonal packing of the hexanuclear metallamacrocycles. Only the part of the alkyl chains (C9 and C10 atoms) are represented in this packing diagram. The disordered hydrophobic alkyl chains of the hexanuclear metallamacrocycles are gathered at the centers of the gigantic hexagonal network.

complex **4**. In the crystal packing structure, the hexanuclear metallamacrocycle **5** serves as a unit for the gigantic hexagonal packing of the metallamacrocycles. The disordered hydrophobic alkyl chains of the hexanuclear metallamacrocycles are gathered at the centers of the gigantic hexagon (Fig. 8).

The charge balance of the metallamacrocycles in the crystal structures suggests that the oxidation state of the manganese ion is $+3$. The oxidation state of the manganese ion is also confirmed by room temperature magnetic susceptibililty measurement. The magnetic moments per metal center in the metallamacrocycles are in the range of 4.55 to 4.83 μ_B. The values correspond to the spin-only value, 4.9, for the high spin manganese(III) d^4 ions.

The methanol solution of the complex **2** in a 3-nitrobenzyl alcohol matrix gave a peak at m/z 1477.6 in the FABMS. This peak corresponds to the hexanuclear metallamacrocycle ion $[Mn_6(ashz)_6 + H]^+$. A similar peak at m/z 1393.5 in complex **1**, corresponding to the hexanuclear metallamacrocycle ion $[Mn_6(fshz)_6 + H]^+$, was previously reported [11]. The solution integrity of the metallamacrocycle was confirmed using paramagnetically shifted ^1H NMR spectroscopy. In the ^1H NMR spectra of all hexanuclear manganese metallamacrocycles in acetone-d_6, three distinctive peaks around -10, -20 and -33 ppm were observed (Fig. 9). These peaks were tentatively assigned to the phenyl protons of the bridging ligands. Similar upfield peaks of the manganese metallacrowns were observed and assigned to the phenyl protons of the salicylhydroximate (shi^{3-}) ligand using deuterium exchange experiments [9g]. The peaks around 38–55 ppm were observed for all complexes with alkyl side chains. The peak at 37.9 ppm was assigned to the methyl protons in the complex **2**, and the peak at 49.9, 54.7, and 53.0 ppm was

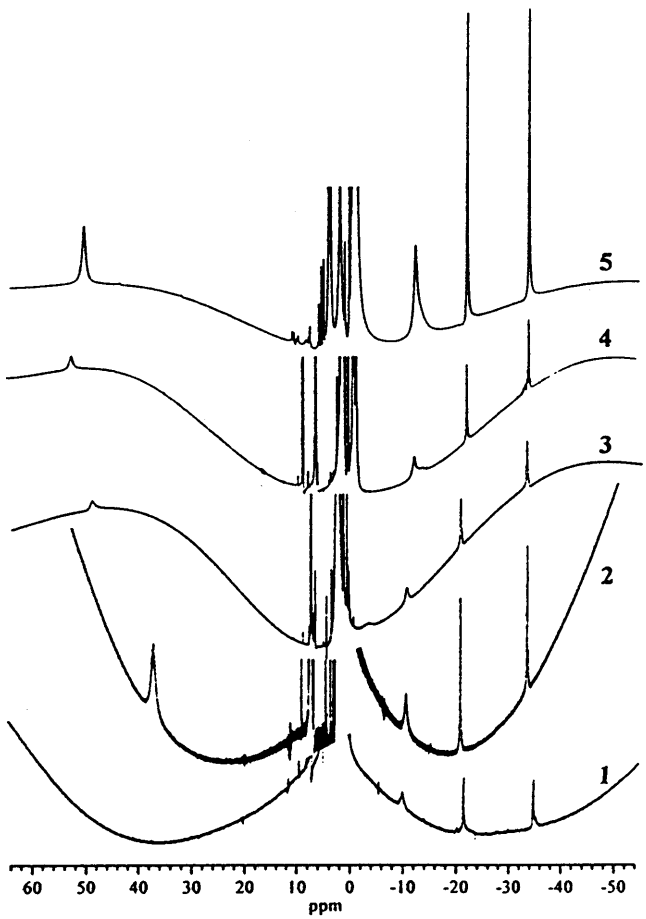

Fig. 9. ^1H NMR spectra of macrocyclic hexanuclear manganese complexes, **1**–**5** in acetone-d_6.

assigned to the methylene protons at the C9 position for the complex **3a**, **4** and **5**, respectively. However, no corresponding peak was observed in the complex **1** (Fig. 9) [11].

All hexanuclear manganese metallamacrocycles with various lengths of hydrophobic aliphatic linear chains are isostructural. The introduction of the side chain to the ligand does not disturb the formation of the hexanuclear manganese metallamacrocycle. Depending on the ligand used, two sets of triple hydrophobic tails of different lengths aligned at a right angle to the plane of the metallamacrocycle in opposite directions to each other. In general, the metallamacrocycle is only slightly soluble in various organic solvents. This might come from the large molecular weight of the metallamacrocycle. However, the solubility of the metallamacrocycle with long hydrophobic alkyl side chains is reasonably good in organic solvent. The ligands with the various functional groups might yield the isostructural metallamacrocycles with the interesting functional groups.

All metallamacrocycles are stable in the solid state. Even in solution, the metallamacrocycles were fairly stable. The ^{1}H NMR spectra of the metallamacrocycles did not change for at least a few months. The stability of the metallamacrocycles might come from the formation of the three chelating rings around the metal ions. The variation of the diameters of the holes (Table 3) implies that the metallamacrocycles have some degree of flexibility. Five donor atoms (from two chelating pentadentate ligands) and an additional donor atom (from a solvent molecule) have coordinated each metal center in the metallamacrocycle. In addition to the stability and flexibility of the metallamacrocycles, the presence of the replaceable solvent site suggests that the hexanuclear manganese metallamacrocycles could be used as a building block for the molecular frameworks [14] or a new type of molecular recognition agent.

4. Supplementary material

Crystallographic data (excluding structure factors) for the structure reported in this paper have been deposited with the Cambridge Crystallographic Data Centre, CCDC Nos. 136344 and 136347. Copies of the data can be obtained free of charge from The Director, CCDC, 12 Union Road, Cambridge, CB2 1EZ, UK (fax: +44-1223-336033; e-mail: deposit@ccdc.cam.ac.uk or www: http://www.ccdc.cam.ac.uk).

Acknowledgements

We thank the Korean Institute of Basic Science for elemental and mass spectroscopy analyses, and the National Institute of Technology and Quality, Dr Y. Park and Dr M. Choi, for the use of their X-ray diffractometers. The authors wish to acknowledge the financial support of the Korea Research Foundation (KRF-99-041-D00280).

References

[1] (a) J.M. Lehn, Supramolecular Chemistry: Concepts and Perspectives, VCH, New York, 1995. (b) D.J. Cram, J.M. Cram, Container Molecules and Their Guests, The Royal Society of Chemistry, Cambridge, UK, 1994.

[2] (a) K.N. Houk, K. Nakamura, C. Sheu, A.E. Keating, Science 273 (1996) 627. (b) J.M. Rivera, T. Martin, J. Rebek Jr., Science 279 (1998) 1021. (c) M. Asakawa, P.R. Ashton, R. Ballardini, V. Balzani, M. Belohradsky, M.T. Gandolfi, O. Kocian, L. Prodi, F.M. Raymo, J.F. Stoddart, M. Venturi, J. Am. Chem. Soc. 119 (1997) 302. (d) Y.M. Jeon, J. Kim, D. Whang, K. Kim, J. Am. Chem. Soc. 118 (1996) 9790. (e) S.S. Zhu, P.J. Carroll, T.M. Swager, J. Am. Chem. Soc. 118 (1996) 8713. (f) M. Berger, F.P. Schmidtchen, J. Am. Chem. Soc. 118 (1996) 8947. (g) C.F. van Nostrum, R.J.M. Nolte, J. Chem. Soc., Chem. Commun. (1996) 2385.

[3] (a) M. Fujita, O. Sasaki, T. Mitsuhashi, T. Fujita, J. Yazaki, K. Yamaguchi, K. Ogura, J. Chem. Soc., Chem. Commun. (1996) 1535. (b) P.J. Stang, B. Olenyuk, Acc. Chem. Res. 30 (1997) 502. (c) R.V. Slone, J.T. Hupp, C.L. Stern, T.E. Albrecht-Schmitt, Inorg. Chem. 35 (1996) 4096. (d) R.V. Slone, D.I. Yoon, R.M. Calhoun, J.T. Hupp, J. Am. Chem. Soc. 117 (1995) 11813.

[4] M.F. Hawthorne, Z. Zheng, Acc. Chem. Res. 30 (1997) 267.

[5] H. Rauter, E.C. Hillgeris, A. Erxleben, B. Lippert, J. Am. Chem. Soc. 116 (1994) 616.

[6] (a) M.J. Hannon, C.L. Painting, A. Jackson, J. Hamblin, W. Errington, J. Chem. Soc., Chem. Commun. (1997) 1807. (b) P.N.W. Baxter, J.M. Lehn, K. Rissanen, J. Chem. Soc., Chem. Commun. (1997) 1323.

[7] M. Clemente-León, E. Coronado, J.R. Galán-Mascarós, C.J. Gómez-García, J. Chem. Soc., Chem. Commun. (1997) 1727.

[8] (a) W. Clegg, A.M. Drummond, R.E. Mulvey, P. O'Shaughnessy, J. Chem. Soc., Chem. Commun. (1997) 1301. (b) F.S. McQuillan, H. Chen, T.A. Hamor, C.J. Jones, K. Paxton, Inorg. Chem. 36 (1997) 4458. (c) A.E. Pullen, J. Piotraschke, K.A. Abboud, J.R. Reynolds, Inorg. Chem. 35 (1996) 793. (d) Q. Huang, X. Wu, Q. Wang, T. Sheng, J. Lu, Inorg. Chem. 35 (1996) 893.

[9] (a) V.L. Pecoraro, A.J. Stemmler, B.R. Gibney, J.J. Bodwin, H. Wang, J.W. Kampf, A. Barwinski, in: K.D. Karlin (Ed.), Progress in Inorganic Chemistry, vol. 45, Wiley, 1997, pp 83. (b) M.S. Lah, V.L. Pecoraro, M.L. Kirk, W.E. Hatfield, in: R.P. Buck, W.E. Hatfield, M. Umaña, E.F. Bowden (Eds.), Biosensor Technology; Marcel Dekker Inc., 1991; pp. 201. (c) M.S. Lah, V.L. Pecoraro, Comments Inorg. Chem. 11 (1990) 59. (d) B.R. Gibney, A.J. Stemmler, S. Pilotek, J.W. Kampf, V.L. Pecoraro, Inorg. Chem. 32 (1993) 6008. (e) M.S. Lah, M.L. Kirk, W. Hatfield, V.L. Pecoraro, J. Chem. Soc., Chem. Commun. (1989) 1606. (f) V.L. Pecoraro, Inorg. Chim. Acta 155 (1989) 171. (g) B.R. Gibney, H. Wang, J.W. Kampf, V.L. Pecoraro, Inorg. Chem. 35 (1996) 6184. (h) B.R. Gibney, J.W. Kampf, D.P. Kessissiglou, V.L. Pecoraro, Inorg. Chem. 33 (1994) 4840. (i) M.S. Lah, V.L. Pecoraro, Inorg. Chem. 30 (1991) 878. (j) M.S. Lah, V.L. Pecoraro, J. Am. Chem. Soc. 111 (1989) 7258. (k) B. Kurzak, E. Farkas, T. Glowiak, H. Kozlowski, J. Chem. Soc., Dalton Trans. (1991) 163. (l) A.J. Stemmler, J.W. Kampf, V.L.

Pecoraro, Inorg. Chem. 34 (1995) 2771. (m) M.S. Lah, B.R. Gibney, D.L. Tierney, J.E. Penner-Hahn, V.L. Pecoraro, J. Am. Chem. Soc. 115 (1993) 5857. (n) A.J. Stemmler, A. Barwinski, M.J. Baldwin, Y. Victor, V.L. Pecoraro, J. Am. Chem. Soc. 118 (1996) 11962. (o) A.J. Stemmler, J.W. Kampf, V.L. Pecoraro, Angew. Chem., Int. Ed. Engl. 35 (1996) 2841. (p) D.P. Kessissiglou, J.W. Kampf, V.L. Pecoraro, Polyhedron 13 (1994) 1379.

[10] (a) A.J. Blake, R.O. Gould, C.M. Grant, P.E. Milne, D. Reed, E.P. Winpenny, Angew. Chem. Int. Ed. Engl. 33 (1994) 195. (b) A.J. Blake, R.O. Gould, P.E. Milne, E.P. Winpenny, J. Chem. Soc., Chem. Commun. (1991) 1453.

[11] B. Kwak, H. Rhee, S. Park, M.S. Lah, Inorg. Chem. 37 (1998) 3599.

[12] G.M. Sheldrick, Acta Crystallogr., Sect. A 46 (1990) 467.

[13] G.M. Sheldrick, SHELX-97; University of Göttingen, Göttinggen, Germany, 1997.

[14] M. Moon, I. Kim, M.S. Lah, Inorg. Chem 39 (2000) 2710.